Check for updates

"Nano effects": a review on nanoparticle-induced multifarious systemic effects on cancer theranostic applications

Gayathri Ravichandran,[†a] Dokkari Nagalaxmi Yadav,[†a] Sivasubramanian Murugappan,[†a] Sri Amruthaa Sankaranarayanan,[a] Neeraja Revi[b] and Aravind Kumar Rengan [ID] *[a]

The advent of nanotechnology has broadened the scope of technological advances in both medical and industrial applications. Nanotechnology has paved the way for cancer diagnosis and therapy with the conceptual inauguration of this field by Nobel laureate Richard Feynman. Understanding how it works and how it interacts with biological systems has been extensively researched, which is critical in its application. When the size of biomaterial systems is reduced from bulk to nano, the surface reactivity increases at the atomic and subatomic scales. Because extraordinary "quantum effects" are pronounced when materials are reduced to nano sizes, understanding the nano-mediated effects is critical. This review introduces and elaborates on the various effects induced by nanoparticles, particularly in the field of cancer treatment.

1. Introduction

Nanotheranostics has taken numerous steps forward in the field of medicine, particularly cancer research, in order to defeat the deadly disease. Various nanoparticles have been studied in cancer research for a variety of applications, including contrast agents in MRI/CT/PET imaging,[1,2] fluorescent quantum dots in diagnosis,[3,4] drug carriers in mediating active targeting to the tumor site,[5] PPT/PDT agents for photo-thermal and photo-dynamic therapy,[6] hypoxia relieving agents in radiotherapy,[7] and even activating the immune system to ablate cancer.[8] The unique effects, as depicted in Fig. 1 that the various nano-systems encompass directly or indirectly project such effectiveness. The "EPR effect" is a well-known phenomenon that has been used to assess the tumor-targeting ability of nanoparticles.[9,10] Endothelial leakiness, the nano knife effect, the abscopal effect, Ostwald ripening, margination dynamics, and quantum tunneling effects are all observed in nanosystems. In this review, the numerous effects embedded in various nano-platforms have been retrospectively analyzed. Though some nanosystems inherently possess such characteristics, they can also be induced through the use of specific nano-modulations.

2. Synthesis associated effects

2.1. Nucleation and growth

The process of formation of a new thermodynamic phase with low free energy from an initial high energy thermodynamic phase by virtue of organised rearrangement is called nucleation.[11] The hypotheses by Volmer, Weber, Frenkel, Becker and Doring were the initial studies on the classical nucleation theory (CNT), the first model trying to understand the kinetics of nucleation.[12–14]

LaMer's model which supplements the CNT came next. It states that initially, the system needs to have a supersaturation level above the critical supersaturation threshold for continuous conversion of precursors to nuclei (nucleation). When the rate of nuclei production exceeds that of precursors, there starts spontaneous growth.[15,16] This further can take various paths of coalescence, monomer addition or Ostwald ripening.[17] But nowadays there are a lot of studies postulating non-classical nucleation and growth, where the energy levels lie between the maximum and minimum.[18] This one parameter can play a major role in deciding the nucleation kinetics of systems. So, in the remaining part of this section, we'll be discussing various parameters affecting nucleation and *vice versa*. Having control over these parameters will help in achieving particles with desired properties.

Usually, in the case of bimetallic particle nucleation, either one of the metal particles must have an inherent property to nucleate itself and act as a nucleation site for the other metal. But the article by Krishnan *et al.* shows a new nucleation method by which bimetallic nanoparticles can be formed with

[a] Dept. of Biomedical Engineering, Indian Institute of Technology Hyderabad, India. E-mail: aravind@bme.iith.ac.in
[b] Dept. of Biotechnology, Indian Institute of Technology Hyderabad, India
† Equal contribution.
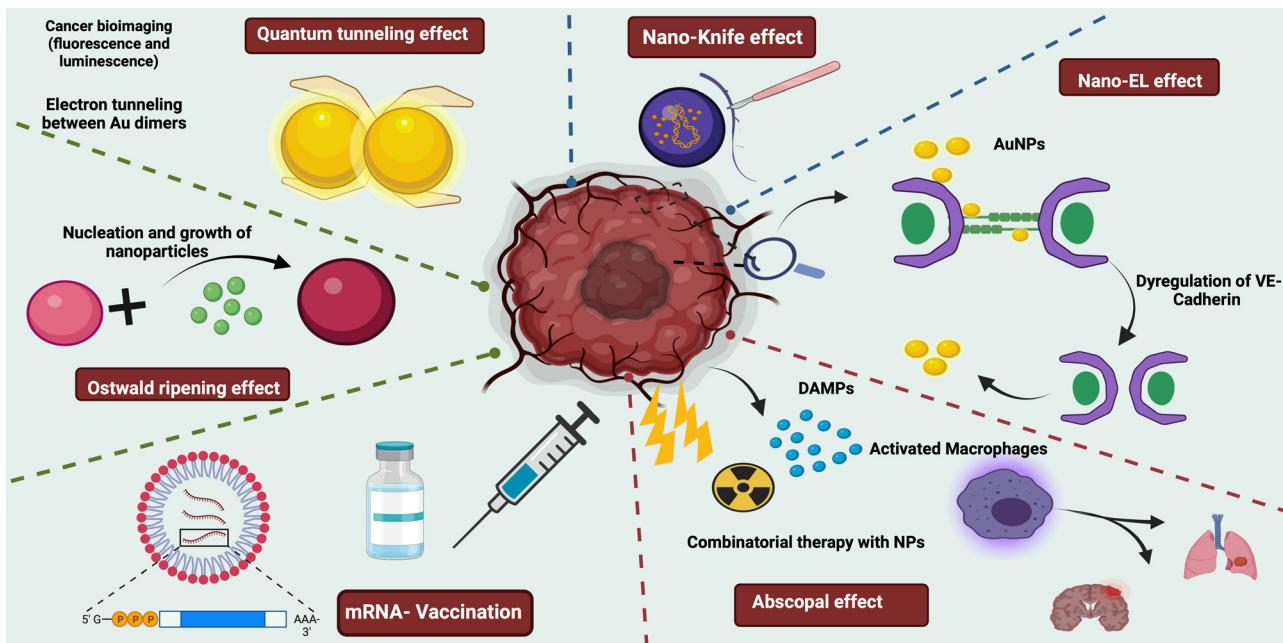
Fig. 1 Schematic representation of various nano-mediated effects on cancer imaging and therapeutics.

a case study of magnesium–titanium (Mg–Ti). This study proposes H_2/CH_4 gas addition as nucleation agents. Experimentally, they have also altered the gas's parameters to control the nucleation rate, size and morphology of the NPs formed. This ability of H_2/CH_4 is due to the dimer bond energies of the bimetal formed and the vapour pressure of the metals involved.[19]

As a result of electrochemical Ostwald ripening, the growth mechanism of Au over MoS_2 nanoflakes lies between diffusion-limited and reaction-limited. The sulphur vacancies in the system support the creation of strong nucleation sites, promoting coalescence and diffusion of Au NPs.[20]

The study by Stevchenko et al. demonstrates that even on heating no Ostwald ripening was observed and the size of CoPt3 NPs was controlled by varying the kinetics of nucleation. Slower nucleation results in large sized particles with less standard deviation (7%) and faster nucleation results in small sized particles with comparatively higher standard deviation (14%).[21] The work of Acharya et al. was also on similar lines indicating that the rate of nucleation is independent of reaction temperature but is dependent on the concentration of free ligands in silver NPs.[22]

Palladium NP growth in a block copolymer micellar template was studied by Parent et al., they found that after monomer addition based nucleation, the system followed aggregation and coalescence, which was later adjusted to get mesoporous NPs.[23,24] But the work of Laramy et al. states that precursors need not necessarily be acting as a seed (template for NP growth). It can also act as a catalyst favouring homogeneous nucleation making it reaction dependent. This in turn suggests that catalytic precursors can not only affect the product morphology but the product nucleation pathway too.[25]

Mozaffari and colleagues inferred that the NP surface and metal precursor play important roles in the nucleation and

growth of NPs and thereby their size too. They have also come up with a new model to predict the size of NPs which involves only the nucleation and growth ratio data.[26] When micelles were slowly added with NaOH in situ, an amorphous precursor phase was formed. This was due to the surface's contrast change. Further addition of NaOH led to nucleation of iron oxide on the micelles, while no nucleation was seen in the bulk outside of the micelles.[27]

Li et al. developed polyaniline NPs, and on observation of its nucleation, it was found that homogeneous nucleation led to nanofibers while heterogeneous nucleation led to granular nanoparticles clearly showing its role in deciding the morphology. Also, surface nucleation led to coral-shaped NPs. Nucleation not only affects the morphology but also aggregation. Continuous vigorous stirring of the reaction solution resulted in aggregation and thereby larger particles. Furthermore, the group has proposed a new aggregation mechanism wherein suppression of heterogeneous nucleation will give small uniform particles without aggregation. In addition, an increase in reaction temperature favours homogenous nucleation, again contributing to the aggregation of particles. This holds true not only for polyaniline NPs but also for silica NPs, attesting to the mechanism's universality.[28]

With all said, there is still a need for better analytical equipment to study nucleation and growth, which will lead to a better unambiguous understanding of the same.[29]

2.2. Aggregation

Physical particle surface contact and reaction induced thermodynamic interactions between colloidal particles are the reason for aggregation to occur. Thermodynamic reactions of nanoparticles in the long range occur by Brownian motion while the short-range ones usually follow the DLVO theory. It states that

the sum of attractive and repulsive forces decides the aggregation. But there are numerous factors involved in deciding the aggregation and vice versa.[30–32]

The work by Keller *et al.* states that adsorption of natural organic matter (NOM) over the nanoparticles leads to the transition of reaction-limited clustered aggregation (RLCA) to diffusion-limited clustered aggregation (DLCA) resulting in reduced aggregation as the electrophoretic mobility values move towards -2 to -0.8 $\mu m\ s^{-1}\ V^{-1}$.[33] A study by Zhang and co-workers infers that the chelation effect of multidentate adsorbates is the primary reason for the stabilized formation of the gold nanoparticles even while FTIR results suggest that alkyl chains contribute to aggregation prevention in the developed Au NPs.[34]

Rojas *et al.* studied the effects of aggregation in magnetic nanoparticles based on the magnetic susceptibility values. Maghemite particles coated with a citrate acid layer showed variations in agar solution due to aggregation but remained unaffected by aggregation within the cell. But again, the *in vivo* results showed varied aggregation and also an alteration in the magnetic properties.[35]

The nanomaterial shape plays a pivotal role in the aggregation. It was validated by Afrooz and group, when they studied polyacrylic acid coated Au nanospheres and Au nanorods of similar electric surface potential and size. From the study, it was found that Au nanospheres showed low critical coagulation concentration (CCC), indicating higher aggregation than Au nanorods.[36] When the surface charge is at the isoelectric point, the aggregation is optimal. The shift in surface charge on either side of the isoelectric point leads to unfavourable aggregation regimes, sometimes irreversible too.[37]

Aggregation not only affects processes indirectly by altering various properties and stimuli but directly too. The study by Sadhukha *et al.* shows that superparamagnetic iron oxide nanoparticles (SPIONs) having uniform particle distribution resulted in conventional hyperthermia while aggregated SPIO NPs led to oxidative stress generation, finally causing a temperature dependent autophagy.[38] Furthermore, the group of Town *et al.* developed an *in situ* forming implant where the colloidal solutions form into a microgel due to aggregation.[39] Similarly, a few fluorescent particles have the ability to exhibit high fluorescence on aggregation, called aggregation induced emission, which are widely used in bioimaging and photodynamic therapies.[40]

2.3. Ostwald ripening (OR)

Ostwald ripening (OR) is a phenomenon caused by a material's ability to maintain a low surface energy state. Smaller solute samples tend to aggregate into the surface of relatively larger particles in a solution containing both solute and solvent, increasing the surface area and achieving a lower energy state. Historically, this was thought to be a barrier to synthesizing and maintaining uniformly sized particles in solutions. However, OR is now thought to be an effective method for the self-controlled synthesis of nanostructures *via* seed elongation or grain growth.[41–45] Ostwald ripening is a key player in the creation

**NUCLEATION AND GROWTH OF PARTICLES**
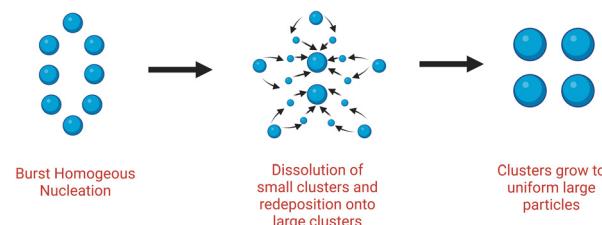
Fig. 2 Schematic illustration of nucleation and growth of nanoparticles leading to Ostwald ripening. Adapted from ref. 47.

of optically superior nanoparticles for use in sensors, circularly polarized luminescence sources, and other applications. Enantiopure mercury sulfide nanoparticles with increased optical activity were synthesized using this method, in which a chiral HgS nanoparticle was prepared alongside a transient achiral HgS nanoparticle, allowing the growth of chiral HgS nanoparticles with 75% increased optical activity.[46] Ostwald ripening was also recently used to create a nanoparticle conjugated Zirconium-based metal organic framework (MOF) capable of dual FRET-induced singlet oxygen generation with near-infrared light[47] (depicted in Fig. 2).

Ostwald ripening also contributes to the production of better gold nanoparticles for surface enhanced Raman spectroscopy (SERS). SERS performance is improved by gold nanoparticles with a rough shape and sharp tips. Ostwald ripening is a process in which Cu ions are used at low concentrations to generate quasi gold nanoparticles around 70 nm and trioctahedral nanoparticles around 200 nm, which interact and form a final product with desired "hot spot" properties for SERS.[48]

Single-crystal lithium niobate ($LiNbO_3$) is used in ferroelectrics, piezoelectrics, and nonlinear optics. The synthesis of $LiNbO_3$, also known as the silicon of photonics, necessitates heat treatment and an inert atmosphere. However, using Ostwald ripening, uniform nanoparticles of $LiNbO_3$ were synthesized through an initial agglomeration reaction followed by surface attachment to form uniform sized crystals.[49]

Ostwald ripening was originally thought to be caused by the inactivation of nanomaterials. It is known for the growth of smaller nanoparticles at the expense of larger (relatively) nanoparticles *via* intermediate chemical states. Smaller nanoparticles are more soluble in emulsions or solutions, so to slow down the rate of solubility, particles tend to aggregate in between the pores of larger particles or stick to the surface *via* outer atomic level interactions. However, with recent evidence favouring the positive exploitation of this physical phenomenon, significant research is required to productively utilize the benefits.

2.4. Quantum tunnelling phenomena

Plasmonic nanomaterials have innate abilities that have been investigated for bioimaging and biosensor applications. They are also extensively researched and explored in the field of cancer diagnosis.[50] When materials are reduced to nanoscale

levels, their quantum effects become more pronounced, and quantum effects such as the quantum tunnelling effect play an important role in fluorescence-based detection. Quantum tunnelling is a phenomenon that occurs between two nanoparticles with interparticle spacings of less than a nanometer. In such a case, electrons tunnel through the space where the electron densities overlap, causing fluorescence to be quenched.[51] As a result, it is critical to investigate tunnelling effects and determine the optimal nanogaps for enhanced fluorescence imaging, as tunnelling has a strong influence on the optical behaviour of various nanosystems. These effects were investigated using TD-DFT calculations. Similarly, level matching induced surface resonant quantum tunnelling (LM-SQRT) is required for the NPES (nanophotonic energy storage) effect to exhibit long-lived or persistent luminescence.[52] Even after the irradiation is turned off, these nanomaterials can emit ultra-long-lived luminescence due to the recombination of trapped charge carriers. The number of traps and their depth in the nanosystem determine the intensity and duration of the effect. Though the intensity is determined by the recombination of the released electrons, the persistent luminescence is caused by the electrons' slow

tunnelling rate. Another fascinating application of quantum tunnelling magnetization (QTM) is seen with GaN:Mn nanoparticles.[53] At the materials' nanoscale, the surface anisotropic field becomes very strong, resulting in a disordered spin state and a channel for quantum tunnelling.

3. Nano-bio interaction-based effects

3.1. Margination dynamics

The design of nanocarriers for drug delivery has been extensively modified over the years to suit the application. The scientific community has investigated the optimal size range, material composition, surface specific modifications, and so on for increasing the efficacy of specific drug-loaded nanocarriers. Margination dynamics, on the other hand, appeared to have been long simplified or ignored until recent years, when several studies, particularly *in silico* and microchannel models, attributed significance to the same.[54–56]

Margination dynamics investigates how the shape of a nanocarrier can influence its adhesion to blood vessels and thus reduce the total site-specific deliverable.[62] The migration of particles towards the walls of a vessel, which is influenced by blood flow rate and its components, has been experimentally validated in a variety of scenarios. It is aided by the hydrodynamic interaction between the vessel walls, which favours RBCs in the vessel's centre. This creates a free space between the RBC-filled centre and the wall, enhancing particle margination. The competitive lift force, which is a perpendicular force acting on materials in a fluid, influences the position of materials in a wall. The greater the lift force, the more centrally the particle will be positioned in a vessel.[62] The influence of various parameters of nanoparticles on margination dynamics is depicted in Fig. 3 and summarized in Table 1.

Elongated particles, particles with a size distribution greater than microns, have been shown to have greater adhesion properties and are frequently phagocytosed. Particles smaller than 20–30 nm are frequently eliminated quickly. As a result, it is critical to comprehend the optimal size and shape in order to maintain increased circulation time while also exhibiting prominent marginal dynamics. Studies comparing different size ranges and shapes of particles with multiple hematocrit values in 2D and 3D models show that spherical particles less than

Factors influencing Margination Dynamics

Particle Shape
Particle Size
Particle Stiffness
Shear Stress and Shear Rate
Hematocrit Composition
Lift Force
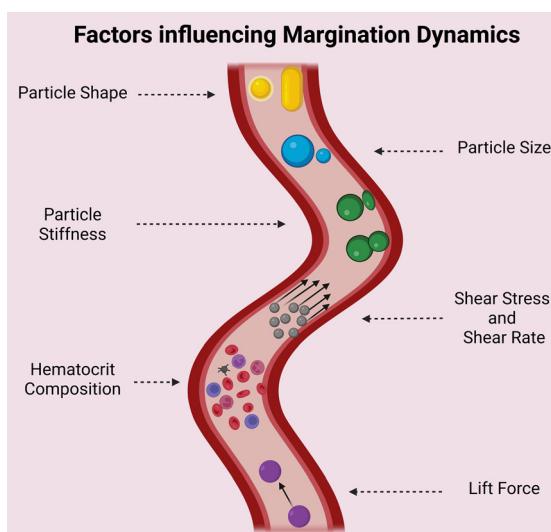
Fig. 3 Effect of various parameters of nanoparticles on margination dynamics.

Table 1 Various factors contributing to margination dynamics

S. No.	Factor	Inference
1	Particle size	Most publications discuss about an ideal size of nanocarriers within the range of 100–200 nm. This range is well enough to ooze out to capillaries and not obstruct the flow like higher sizes in microns[56,58–61]
2	Particle shape	Ellipsoid particles tend to have a larger surface area for attachment. However, the same is valid only when the larger side comes into contact with the endothelium. However, due to tumbling they may come into interaction with RBCs and hence experience drag and reduction in margination[62]
3	Particle stiffness	Collision between a stiff and elastic carrier can cause margination[63]
4	Hematocrit composition	Affects the boundary of the RBC free layer (RBCFL)[64]
5	Lift force	Determines the RBCFL width paving the way for particle margination[65]
6	Shear rate	RBCFL thickness grows with increased shear rate. Under higher shear rate ellipsoid particles binds more to the walls than spherical particles. A transition shear rate region is there for spherical and ellipsoid microparticles where margination probability dramatically increases with the shear rate lesser than this region and slowly grows above this region[66,67]

200 nm and above 100 nm have less margination than ellipsoid particles of the same area, owing to the latter's slower rotation time near the walls and larger surface area for adhesion.[57,64–66]

Marginal dynamics is of great significance when it comes to cancer therapy and diagnostics. Particles moving close to the vessel walls will increase the probability of oozing out to nearby capillaries and favours antibody or other ligand specific inter-action with the endothelium. When it comes to imaging, its often preferable for the particle to have lesser margination as it would allow it to stay in the bloodstream for a longer period.[61,69]

3.2. The nanoEL effect

Endothelial leakiness (EL) is an ingrained characteristic of tumor architecture that tailors it into the most aggressive forms by facilitating metastasis and angiogenesis, which is mediated by factors such as vascular endothelial growth factor (VEGF) and histamine. On the contrary, this disruption in blood vessel integrity has been tuned as a beneficial mechanistic approach that drives the passive targeting of nanomaterials in the facet of cancer nanotherapeutics.[68] The increased permeability caused by the leaky vasculature facilitates the passage of administered nanoparticles across the endothelial barrier, culminating in their accretion in the tumor zone.[69] In addition to tumor architecture, nanoparticle density has been shown to influence endothelial leakiness.[70]

In addition to the aforementioned canonical ligand–receptor mediated disruption pathway, Setyavati *et al.*'s study revealed the strong EL effect caused by the administration of nanomaterials. The pull-down assay and the proximity ligation assay were used to confirm TiO_2 nanomaterials binding to VE-Cadherin in endothelial cell adherent junctions. As a result of the coupling, VE-Cadherin and catenin interaction was impaired, resulting in actin remodelling and cell-shape deformation. Surprisingly, the leakiness was found to be size-dependent, with gaps generated only with nano-size TiO_2 NM (23.5 nm) and not with micro-size TiO_2 NM (680 nm).[71]

After demonstrating this fascinating feature, the NanoEL effect, which has the potential to increase nanoparticle accumu-lation in the tumor site, has raised major concerns. This is related to the leakiness observed in other organs as a result of the TiO_2 nanomaterials, which can then serve as a vulnerable site for secondary tumors.[72] Recent *in vivo* experimental evidence supports the concept of metastasis as a result of accelerated intravasation of breast cancer cells through nanometer gaps facilitated by TiO_2, Au, Ag, and SiO_2 nanoparticles. The dose-dependent transpiration of metastatic lesions in the lungs, liver, and bone muscles is confirmed by the quantification of biolu-minescent images of harvested organs. This inherent property of nanomaterials to induce endothelial leakage, on the other hand, can be leveraged therapeutically for the passage of nanomedicines across the blood–brain barrier (BBB).[72] Though the NanoEL effect provides the accessibility to immature tumors in the absence of an EPR effect, much more research is required in optimizing the size and sensitivity of endothelial cells of different origins to these nanoparticles to ensure off-target nanotoxic adverse side effects.

3.3. The nanoknife effect

Graphene's two-dimensional honeycomb lattice structure is made up of tightly packed single carbon atoms. Graphene-based nanomaterials have been used in a variety of therapeutic applications, including drug delivery, diagnostics, antimicrobial properties, biosensing, tissue scaffolds, and so on. The benefits that support the broad applicability include low toxicity, bio-compatibility, reproducibility, and flexibility for innovative func-tionalization. Another such distinct therapeutic property of graphene nanosheets was identified by Akhavan *et al.* in their study a decade ago, and was later dubbed the nano-knife effect. This first study examined the underlying toxicity mechanism effectuating antibacterial effects by comparing graphene oxide nanosheets (GONS) and reduced graphene nanosheets (RGNS).[73]

Bacterial inactivation upon direct contact with the cell membrane was attributed to the sharp edges of the GNS, as well as the improved charge transfer bound by the two entities. Damage to the cell membrane caused by the nano knife effect was more pronounced in RGNS than in GONS, as measured by the extent of RNA efflux. The strong interaction exhibited by the enhanced sharp edges of the reduced GNS was attributed as the cause.[74] In accordance with the rationale, experimental and computational studies were conducted in tandem to further entail the understanding of the nano knife effect.[75] The study hypothesized that the bacterial cell's viability was hampered by the reduced osmotic pressure caused by the localized piercing of the GNS, which caused swelling and death. Single chain main field (SCMF) simulations revealed the significance of GN lipophilicity in the formation of pores by analysing the eventful interactions between GNS and the cell membrane, instigating the nano knife effect. This mechanism is also known as insertion mode or penetration mode, and it results in the efflux of intracellular components.[76] Another study reported the development of zinc-doped copper oxide nanomaterials for a potential anti-bacterial effect. Though several studies have reported the use of Zn and Cu based nanomaterials for anti-bacterial effects, the relationship between the nanostructure and its role in bacterial killing is underexplored. In this study, Zn–CuO with prickly nanostructures was found to exhibit a very strong anti-bacterial activity with killing of 99% in comparison with Zn–CuO nanorods *via* an "architecture-enhanced nano piercing" of the bacterial membrane[77] (depicted in Fig. 4).

The nanoknife effect was then extended to cancer therapeutics *via* utilizing the ablative nature of the technique in creating small pores (irreversible electroporation) in the cancer cell membrane, thereby causing permanent damage to cancer cells. Convention-ally, nanodiamonds (layers of graphite) were fabricated and their popcorn-like structural confirmations were induced by photoly-sis, and they have been tested for their nanoknife effect against lung cancer A549 cell lines. The fabricated nanodiamond was coupled to a cancer cell specific growth hormone (GH), an NDGH complex, which was reported to specifically eliminate cancer cells upon pulsed high energy laser irradiation. The high affinity of NDGH to cancer cell membranes coupled with the ND explosion upon irradiation ended up in damaging the cell membrane *via*
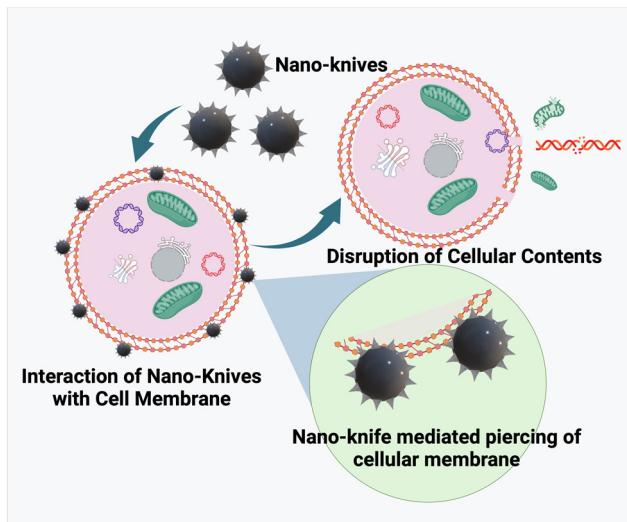
Fig. 4 Mechanism of nano-knife mediated killing of cells.

localized uncovering of high energy.[78] Two-dimensional nanosheet-like structures of tungsten, black phosphorous, titanium, *etc.* have been developed for potential use as nanoknifes in cancer treatment. Recently, copper sulfide (CuS) based NIR II responsive nanosheets were developed for NIR II PTT. The surface functionalization with cysteine helped as a template as well as sulphur resource to form Cys-CuS nanosheets. The developed nanosystem exhibited remarkable NIR II mediated PTT performance in an ultrashort time (irradiation time of 40 s), thereby proving to be a promising biocompatible nanoknife in combination with PTT to significantly reduce the surgery time with minimal side effects.[79] A specialized device, generally made of graphene/carbon nanotubes is employed for generating short pulses of high voltage electric current within the cell membrane. The nano-knife has emerged as a revolutionary tool in cancer theranostics owing to its minimal invasiveness and spatial-control based specificity.[80,81] Such architecture-mediated cell membrane piercing would pave the way for the design and development of several nanostructures for efficient and specialized therapeutics for infections and tumor elimination. However, more research is required on the targeting ability, toxicity, clearance, and blood–nanoparticle interaction of these materials to overcome off-target toxicities and adverse side effects.

3.4. Abscopal effect mediated by multifunctional NPs

Cancer metastasis, which accounts for more than 90% of all fatalities, is a major concern, and therapeutic strategies that can reduce the fatality rate are widely recognized.[82] In this regard, when localized therapy was administered at the primary tumor site, a unique effect was observed in a patient with the shrinkage of metastatic lesions. This offsite effect caused by secondary tumor sites was dubbed the abscopal effect, which was first described by R. H. Mole in 1953 and means "away from the target" in Latin. The awakening of the immune system was thought to have triggered the abscopal effect. Because this effect was a rare occurrence in the context of radiotherapy, research was escalated with a strategic approach to make it

more reliable.[83] The sequential process that occurs in this effect begins with the application of any localized therapy, after which dying cells release DAMPS, which activates DC. This is followed by an influx of CD8+ and CD4+ T cells (depicted in Fig. 5). Tumor hypoxia, as a limiting factor, creates a tumor microenvironment with a dysfunctional immune response due to the infiltration of immunosuppressive cells such as Treg and MDSCs. Furthermore, T cell exhaustion is a phenomenon that is mediated by CTLA-4 and PDL1/PD1 activation. In order to elicit immunogenic cell death, various immune checkpoint inhibitors (ICIs) have been used to overcome these barriers.[83,84]

Nanoparticles have been studied for the targeted delivery of payloads, and they have been shown to enhance the abscopal effect in a variety of ways.[84] Min and colleagues created a functionalized PLGA nanoparticle that efficiently captures neoantigens released by dying tumor cells. As a result, dendritic cell uptake of these AC-NPs improves antigen presentation and immune activation in the draining lymph nodes. As a result, the T repertoire migrates to the unirradiated secondary tumor to mediate ICD. The immune response can be boosted further by recognizing the hypoxic tumor microenvironment and implementing strategies to alleviate oxygen tension.[85] As a result, Chen *et al.* combined ionizing radiation beams with catalase encapsulated in PLGA nanoparticles, which redistributes oxygen in the tumor region by converting H_2O_2 to O_2 in order to moderate the tumor microenvironment. These NPs were also loaded with R837 adjuvant in hydrophobic PLGA pouches, which results in a strong anti-tumor immune response.[86] This study also includes checkpoint blockades *via* anti-CTLA-4, which synergistically elicits the whole-system abscopal effect and produces long-term memory.

Other treatment regimens, such as photodynamic therapy and photothermal therapy, have also made a significant contribution to the abscopal effect.[87] As an example, Chen *et al.* created a hybrid protein nanocarrier by encapsulating it with chlorine e6 and using HAS and Hb as efficient oxygen carriers. Flow cytometry and the IF assay revealed a two-fold increase in CD8+ T cell infiltration in the tumor, resulting in a 73% inhibition of lung metastasis. In the aforementioned studies,
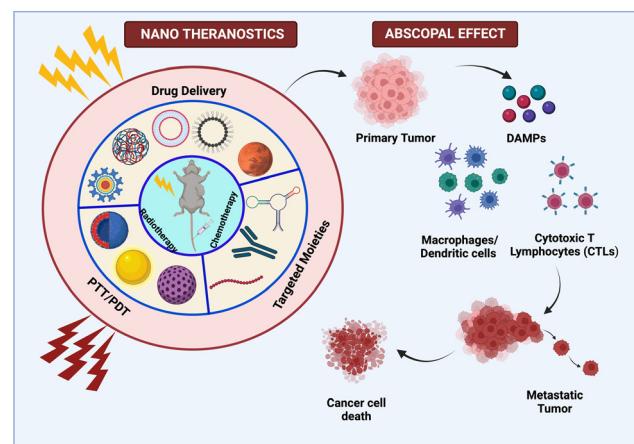

Fig. 5 Multifarious nanosystems eliciting abscopal effect as a combinatorial therapy with radiotherapy and immunotherapy.

nanoparticles significantly augmented the abscopal effect by modulating the tumor hypoxic microenvironment, transporting TDPAs to APCs, and targeting the delivery of combinatorial therapeutic ingredients such as checkpoint blockade inhibitors, oxygen delivery, photosensitizers, adjuvants, and so on, all of which synergistically triggered a systemic abscopal effect.

3.5. The EPR effect: the fundamental tenet of nanoengineering

The two abnormalities that lay the groundwork for the EPR effect of nanoparticles in tumor vasculature are leaky vasculature and faulty lymphatic drainage.[88] Two independent research groups (Jain and Maeda) demonstrated tumor homing of proteins and dyes in 1986. Two years later, using electron microscopy, the Jain group documented the permeability of blood vessels in the tumor zone, which results in nanoparticle extravasation. The presence of open gaps in the inter-endothelial junctions was attributed to this. The NanoEL effect has been used to explain the formation of endothelial gaps. Since then, the EPR effect has served as a guiding principle in the development of nanoparticles for the passive delivery of therapeutic ingredients (depicted in Fig. 6). However, the intriguing question here is about the properties of nanoparticles that can cause the EPR effect. Due to the size of gaps ranging up to 2000 nm,[89] size has been one of the many and foremost fundamental criteria used while designing. Charge, surface chemistry, and shape are examples of physical characteristics.[90,91]

The half-life of nanoparticles in blood circulation also has a significant impact on the overall fate of nanoparticle extravasation into tumors *via* the EPR effect. The half-life can vary greatly depending on protein adsorption, which can form a hard or soft protein corona layer, non-specific uptake by the liver and spleen, and subsequent degradation by the MPS.[92] As a result, an NP's chemo-physical properties play a significant role in these aspects that govern its fate. The first generation of nanoparticle design was governed by tuning the size of nanoparticles less than 100 nm and larger than this size, which resulted in unsuccessful tumor homing. Size also plays a role in increasing the half-life of nanoparticles, with sizes larger than

200 nm being captured by MPS cells. The surface charge of nanoparticles is another major factor influencing EPR, with positively charged NPs causing unintended uptake by the liver and spleen while negatively or neutral nanoparticles are well tolerated.[93] After successful extravasation, intra-tumoral pressure (IFP) and dense extracellular matrix (ECM) strongly regulate nanoparticle retention.[94] Dense collagen fibers in the interstitial tumor extracellular matrix not only impede nanoparticle diffusion, but because they are slightly positively charged, they tend to aggregate with negatively charged nanoparticles.[95] In such cases, cationic nanoparticles can solve the problem. With such contrasting patterns portrayed by positively and negatively charged nanoparticles, smart nanoparticles have been developed that switch their surface charge from negative in blood circulation for extended half-lives to positively charged once they reach the tumor interstitial space. Overall, effective particle modulation is significant and could synergistically increase its half-life, allowing more particles to be spared for the EPR effect of nanoparticles.[96]

Surprisingly, recent evidence revealed the rare occurrence of gaps in endothelial junctions and the existence of another transportation route for nanoparticle extravasation. By conducting five different experiments to determine the dominant mode of nanoparticle extravasation, this study yielded fascinating key findings. The Zombie model developed by the W. C. Chan group explicitly demonstrated that the transfer of NPs through the vessel was actively supported by the trans-endothelial route, which was further reinforced by intravital microscopy for real-time capturing of dynamic changes.[9] Despite the fact that a few nanodrugs have been approved for use in clinics, they are still plagued by low efficacy. This reinforces the notion that understanding nano-bio interactions is critical for increasing the efficacy of clinically implemented nanoformulations for improved treatment outcomes.

3.6. Messenger RNA (mRNA) vaccination for nanoparticle-mediated therapy

DNA is involved in the transcription of genetic information from genes into messenger RNA (mRNA), while mRNA is involved in the translation of genetic information into proteins. The origin of mRNA can be exogenous or endogenous.[97,98] The exogenous mRNA is produced outside the cells and can be delivered into the cell cytosol.[97] mRNA vaccines use such mRNA to produce antigen proteins of interest within the ribosome and develop an immune response against pathogens and cancer cells.[99,100] The current clinical trials for mRNA as a therapeutic agent are mostly focused on vaccination, cancer immunotherapy, and protein replacement therapy.[101,102] mRNA-mediated transfection provides a compelling alternative to plasmid DNA (pDNA)-based gene therapy,[97] as pDNA produces proteins even in non-dividing cells and it is difficult to transfect cells without the hazards of genomic integration and insertional mutagenesis.[98,99] In contrast, mRNA vaccines do not require crossing nuclear barriers to function, they do not offer a danger of genomic integration and insertional mutagenesis and they also boost immune responses.[99,103] The mechanism of mRNA NP mediated cancer therapy is depicted in Fig. 7.
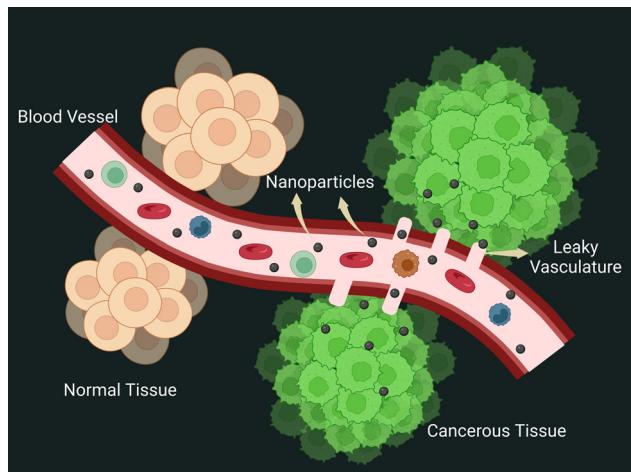
Fig. 6 Schematic depicting the EPR effect.

Wolff *et al.* developed gene-based vaccination in 1990 for the 1st time. In this study, they have shown the expression and uptake of introduced exogenous pDNA and also its transcription into mRNA through *in vitro* studies.[103] In 1997, the first clinical experiment employing mRNA was undertaken, in which transfected dendritic cells were used to stimulate an immunological response in cancer patients.[98] Researchers utilized the full tumor mRNA to vaccinate melanoma cancer patients once more in 2008.[98] Thus, using mRNA as a vaccine can help patients to develop an immune response to detect the tumor cells and produce a cell-mediated antitumor effect.[104,105] mRNA vaccines show more advantages over other proteins and vectors including stability, safety, producibility, long-term storage, and release, and they also generate wide cytotoxic T-cell immune responses.[103,106]

mRNA is roughly 10^5–10^6 Dalton in size, which is 3–4 times bigger than the other molecules that diffuse the cells. It repels the anionic cell membrane because of its cationic charge.[101] However, due to stability difficulties, degradation by RNases present in bodily fluids, poor cellular uptake, and immunogenicity limit its uses.[98,103] So, mRNA-mediated treatment has not been employed as a therapeutic agent for a longer period of time, limiting its application for *in vivo* research.[103,107] Thus, effective targeted delivery can be achieved by protecting the mRNA using a proper carrier.[98] Currently, lipid and polymer-based nanoparticles are used as a carrier to deliver mRNA to the tumor location.[103,105,108] These nanoformulations are safer and protect the mRNA from degradation, immunogenicity and toxicity, and enhance cellular uptake, undergo endosomal escape, and release the therapeutic agents into the cytosol.[109]

For example, Xingfang Su *et al.* developed lipo-polymeric nanoparticles consisting of a pH-responsive poly-(β-amino ester) (PBAE) polymeric core encapsulated with a phospholipid shell. The negatively charged mRNA is held together by adsorption *via* ionic interactions onto the surface of positively charged nanoparticles. These particles have protected the mRNA from degradation and undergo endosomal escape bursting the endosome and releasing the components into the cytosol of dendritic cells with lower toxicity. When these particles were given

intranasally to mice, effective mRNA delivery was observed. So, these particles might be useful for the non-invasive administration of mRNA-based vaccinations.[103] Similarly, redox-responsive lipo-polymeric nanoparticles were developed by Na Kong *et al.* to deliver exogenous therapeutic p53 mRNA while shielding it from nuclear localization and insertional mutagenesis. By causing cell death and G1-phase cell cycle arrest, these particles have demonstrated an anticancer effect *in vitro* and *in vivo*.[110]

In a study, Mohammad *et al.* developed an ovalbumin-coded mRNA antigen for a vaccination with Resiquimod drug (R848) that had been chemically altered to enhance the immune responses and therapeutics. These particles underwent additional palmitic acid modification before being coated in lipid-polyethylene glycol to improve their encapsulation efficacy. These vaccines demonstrated improved MHC class I antigen presentation in antigen-presenting cells *in vitro*, better transfection efficiency, and enhanced antigen-specific CD8+ T cell responses *in vivo*. Thus, these exogenous mRNA vaccines serve as an antigen source to activate a positive anti-tumor response mediated by CD8+ T lymphocytes.[111]

In a study, Tongren Yang *et al.* developed ionizable lipid nanoparticles to carry two distinct mRNAs erythropoietin and luciferase that are generated *in vitro* by transcription and decorated with poly (A) tails and anti-reverse cap analogs (ARCA). These particles exhibit improved encapsulation efficiency, efficiently transfer mRNA to the cells, and accomplish *in vitro* and *in vivo* protein expression.[112] Similarly in a study, M. Margaret *et al.* developed an ionizable lipid nanoparticle for mRNA-based *ex vivo* engineering of CAR T cells. In comparison to commercially available lipofectamine, these particles improved chimeric antigen receptor (CAR) mRNA distribution to human T cells (Jurkat cells) and also reduced cytotoxicity.[113]

In another study, utilizing heterocyclic lipids, Lei Miao *et al.* created ionizable lipid nanoparticles that improved the intracellular transport of mRNA to the targeted locations by employing the stimulator of interferon genes (STING) route rather than the toll-like receptors through the endocytic mechanism. In *in vivo* tumor models, these particles have also stimulated immune responses and reduced tumor development.[114] In order to transfer *in vitro* generated mRNA by lipid raft-mediated endocytosis, Xueyan *et al.* developed a liposome-protamine lipoplex. Compared to their plasmid counterpart, these particles have demonstrated better transfection and anticancer effects.[115]

Consequently, these exogenous mRNAs along with ionizable lipid nanoparticles can be used as vaccines with different antigens such as tumor-associated antigens, commercial-designed multi-epitope antigens, and viral and bacterial proteins.[114] Thus, it has been suggested that mRNA along with such nanoparticles is a potential therapeutic platform for vaccinations and protein replacement for cancer immunotherapy while overcoming all of the restrictions of delivering naked mRNA.[101,116]

Fig. 7 Mechanism of mRNA nanoparticle-mediated therapy.

4. Conclusion

This review has retrospectively analysed various effects ingrained within the various nano-platforms. Because an

in-depth understanding of nano-bio interactions is required, examining these effects for a specific nanosystem provides more clarity into the therapeutic design. These effects can be modulated within the biological system to achieve the desired functional output. Conversion of bulk biomaterials to nano-sized particles enables higher reaction of the system at the atomic and sub-atomic levels. In other words, it allows us to investigate the spectrum of inherent properties and apply them to cancer therapy. Emerging technologies, such as nanomedicine, are significantly transforming medical care. Nanoparticles are used in a variety of diagnostic and therapeutic applications. Our ability to investigate the full range of inherent properties found in these nanosystems will aid in cancer treatment.

Conflicts of interest

There are no conflicts to declare.

Acknowledgements

References

1 A. Farzin, S. A. Etesami, J. Quint, A. Memic and A. Tamayol, *Adv. Healthcare Mater.*, 2020, **9**, 1901058.

2 D. Luo, X. Wang, C. Burda and J. P. Basilion, *Cancers*, 2021, **13**(8), 1825.

3 S. Iravani and R. S. Varma, *Environ. Chem. Lett.*, 2020, **18**, 703–727.

4 R. D. Singh, R. Shandilya, A. Bhargava, R. Kumar, R. Tiwari, K. Chaudhury, R. K. Srivastava, I. Y. Goryacheva and P. K. Mishra, *Front. Genet.*, 2018, **9**, 616.

5 S. Raj, S. Khurana, R. Choudhari, K. K. Kesari, M. A. Kamal, N. Garg, J. Ruokolainen, B. C. Das and D. Kumar, *Semin. Cancer Biol.*, 2021, **69**, 166–177.

6 M. Yang, J. Deng, H. Su, S. Gu, J. Zhang, A. Zhong and F. Wu, *Mater. Chem. Front.*, 2021, **5**(1), 406–417.

7 H. Wang, J. Li, Y. Wang, X. Gong, X. Xu, J. Wang, Y. Li, X. Sha and Z. Zhang, *J. Controlled Release*, 2020, **319**, 25–45.

8 Z. Yang, Y. Ma, H. Zhao, Y. Yuan and B. Y. S. Kim, *Wiley Interdiscip. Rev.: Nanomed. Nanobiotechnol.*, 2020, **12**(2), e1590.

9 S. Sindhwani, A. M. Syed, J. Ngai, B. R. Kingston, L. Maiorino, J. Rothschild, P. MacMillan, Y. Zhang, N. U. Rajesh, T. Hoang, J. L. Y. Wu, S. Wilhelm, A. Zilman, S. Gadde, A. Sulaiman, B. Ouyang, Z. Lin, L. Wang, M. Egeblad and W. C. W. Chan, *Nat. Mater.*, 2020, **19**(5), 566–575.

10 X. Liu, J. Jiang and H. Meng, *Theranostics*, 2019, **9**(26), 8018.

11 S. Karthika, T. K. Radhakrishnan and P. Kalaichelvi, *Cryst. Growth Des.*, 2016, **16**(11), 6663–6681.

12 M. Volmer and A. Weber, *Z. Phys. Chem.*, 1926, **119**, 277–301.

13 R. Becker and W. Döring, *Ann. Phys.*, 1935, **416**, 719–752.

14 J. Frenkel, *J. Chem. Phys.*, 1939, **7**, 538–547.

15 V. K. LaMer and R. H. Dinegar, *J. Am. Chem. Soc.*, 1950, **72**, 4847–4854.

16 P. W. Dunne, A. S. Munn, C. L. Starkey, T. A. Huddle and E. H. Leste, *Philos. Trans. R. Soc., A*, 2015, **373**(2057), 20150015.

17 N. T. K. Thanh, N. Maclean and S. Mahiddine, *Chem. Rev.*, 2014, **114**, 7610–7630.

18 J. Lee, J. Yang, S. G. Kwon and T. Hyeon, *Nat. Rev. Mater.*, 2016, **1**(8), 1–16.

19 G. Krishnan, S. De Graaf, G. H. Ten Brink, P. O. Å. Persson, B. J. Kooi and G. Palasantzas, *Nanoscale*, 2017, **9**, 8149–8156.

20 B. Song, K. He, Y. Yuan, S. Sharifi-Asl, M. Cheng, J. Lu, W. A. Saidi and R. Shahbazian-Yassar, *Nanoscale*, 2018, **10**, 15809–15818.

21 E. V. Shevchenko, D. V. Talapin, H. Schnablegger, A. Kornowski, Ö. Festin, P. Svedlindh, M. Haase and H. Weller, *J. Am. Chem. Soc.*, 2003, **125**, 9090–9101.

22 A. Acharya, M. Zamkov and A. T. Zayak, Doctoral thesis, Graduate College of Bowling Green State University, 2015.

23 T. J. Woehl, J. E. Evans, I. Arslan, W. D. Ristenpart and N. D. Browning, *ACS Nano*, 2012, **6**, 8599–8610.

24 L. R. Parent, D. B. Robinson, P. J. Cappillino, P. Abellan, J. E. Evans, N. D. Browning and I. Arslan, *Microsc. Microanal.*, 2014, **20**, 1600–1601.

25 C. R. Laramy, L. K. Fong, M. R. Jones, M. N. O'Brien, G. C. Schatz and C. A. Mirkin, *Chem. Phys. Lett.*, 2017, **683**, 389–392.

26 S. Mozaffari, W. Li, C. Thompson, S. Ivanov, S. Seifert, B. Lee, L. Kovarik and A. M. Karim, *Nanoscale*, 2017, **9**, 13772–13785.

27 S. Kashyap, T. J. Woehl, X. Liu, S. K. Mallapragada and T. Prozorov, *ACS Nano*, 2014, **8**, 9097–9106.

28 D. Li and R. B. Kaner, *J. Am. Chem. Soc.*, 2006, **128**, 968–975.

29 R. K. Ramamoorthy, E. Yildirim, E. Barba, P. Roblin, J. A. Vargas, L. M. Lacroix, I. Rodriguez-Ruiz, P. Decorse, V. Petkov, S. Teychené and G. Viau, *Nanoscale*, 2020, **12**, 16173–16188.

30 E. M. Hotze, T. Phenrat and G. V. Lowry, *J. Environ. Qual.*, 2010, **39**, 1909–1924.

31 B. Derjaguin and L. Landau, *Prog. Surf. Sci.*, 1993, **43**, 30–59.

32 J. T. G. Overbeek and E. J. W. Verwey, *Nature*, 1948, **162**(4113), 315–316.

33 A. A. Keller, H. Wang, D. Zhou, H. S. Lenihan, G. Cherr, B. J. Cardinale, R. Miller and J. I. Zhaoxia, *Environ. Sci. Technol.*, 2010, **44**, 1962–1967.

34 S. Zhang, G. Leem, L. O. Srisombat and T. R. Lee, *J. Am. Chem. Soc.*, 2008, **130**, 113–120.

35 J. M. Rojas, H. Gavilán, V. del Dedo, E. Lorente-Sorolla, L. Sanz-Ortega, G. B. da Silva, R. Costo, S. Perez-Yagüe, M. Talelli, M. Marciello, M. P. Morales, D. F. Barber and L. Gutiérrez, *Acta Biomater.*, 2017, **58**, 181–195.

36 A. R. M. N. Afrooz, S. T. Sivalapalan, C. J. Murphy, S. M. Hussain, J. J. Schlager and N. B. Saleh, *Chemosphere*, 2013, **91**, 93–98.

37 J. Zhang and J. Buffle, *J. Colloid Interface Sci.*, 1995, **174**(2), 500–509.

38 T. Sadhukha, T. S. Wiedmann and J. Panyam, *Biomaterials*, 2014, **35**, 7860–7869.

39 A. R. Town, M. Giardiello, R. Gurjar, M. Siccardi, M. E. Briggs, R. Akhtar and T. O. McDonald, *Nanoscale*, 2017, **9**, 6302–6314.

40 Y. Li, R. Tang, X. Liu, J. Gong, Z. Zhao, Z. Sheng, J. Zhang, X. Li, G. Niu, R. T. K. Kwok, W. Zheng, X. Jiang and B. Z. Tang, *ACS Nano*, 2020, **14**, 16840–16853.

41 C. W. Lee, P. C. Wu, I. L. Hsu, T. M. Liu, W. H. Chong, C. H. Wu, T. Y. Hsieh, L. Z. Guo, Y. Tsao, P. T. Wu, J. Yu, P. J. Tsai, H. S. Huang, Y. C. Chuang and C. C. Huang, *Small*, 2019, **15**, 1–11.

42 G. Ferraro and E. Fratini, *J. Chem. Educ.*, 2019, **96**(3), 553–557.

43 X. Cao, L. Zhi, Y. Li, F. Fang, X. Cui, L. Ci, K. Ding and J. Wei, *ACS Appl. Energy Mater.*, 2018, **1**(2), 868–875.

44 W. Wang, S. Zhou, M. Shen, Z. D. Hood, K. Xiao and Y. Xia, *ChemNanoMat*, 2018, **4**(10), 1071–1077.

45 J. Kim, S. W. Lee, M. H. Kim and O. O. Park, *ACS Appl. Mater. Interfaces*, 2018, **10**(45), 39134–39143.

46 J. Kuno, K. Miyake, S. Katao, T. Kawai and T. Nakashima, *Chem. Mater.*, 2020, **32**(19), 8412–8419.

47 Y. Liu, Y. Yang, Y. Sun, J. Song, N. G. Rudawski, X. Chen and W. Tan, *J. Am. Chem. Soc.*, 2019, **141**(18), 7407–7413.

48 C. Wu, H. He, Y. Song, C. Bi, L. Xing, W. Du, S. Li and H. Xia, *Nanoscale*, 2020, **12**(32), 16934–16943.

49 R. F. Ali and B. D. Gates, *Chem. Mater.*, 2018, **30**(6), 2028–2035.

50 J. A. Scholl, A. García-Etxarri, A. L. Koh and J. A. Dionne, *Nano Lett.*, 2013, **13**(2), 564–569.

51 N. V. Ilawe, M. B. Oviedo and B. M. Wong, *J. Mater. Chem. C*, 2018, **6**(22), 5857–5864.

52 M. Sun, H. Dong, A. W. Dougherty, Q. Lu, D. Peng, W. T. Wong, B. Huang, L. D. Sun and C. H. Yan, *Nano Energy*, 2019, **56**, 473–481.

53 Y. Xu, B. Yao and Q. Cui, *RSC Adv.*, 2016, **6**(9), 7521–7526.

54 F. Gentile, C. Chiappini, D. Fine, R. C. Bhavane, M. S. Peluccio, M. M. C. Cheng, X. Liu, M. Ferrari and P. Decuzzi, *J. Biomech.*, 2008, **41**(10), 2312–2318.

55 F. Gentile, A. Curcio, C. Indolfi, M. Ferrari and P. Decuzzi, *J. Nanobiotechnol.*, 2008, **6**, 1–9.

56 P. Jurney, R. Agarwal, V. Singh, K. Roy, S. V. Sreenivasan and L. Shi, *J. Nanotechnol. Eng. Med.*, 2013, **4**(3), 1–7.

57 K. Müller, D. A. Fedosov and G. Gompper, *Sci. Rep.*, 2014, **4**, 1–8.

58 K. Namdee, A. J. Thompson, P. Charoenphol and O. Eniola-Adefeso, *Langmuir*, 2013, **29**(8), 2530–2535.

59 T. R. Lee, M. Choi, A. M. Kopacz, S. H. Yun, W. K. Liu and P. Decuzzi, *Sci. Rep.*, 2013, **3**, 1–8.

60 J. Tan, S. Shah, A. Thomas, H. D. Ou-Yang and Y. Liu, *Microfluid. Nanofluid.*, 2013, **23**(14), 1–2.

61 H. T. Ta, N. P. Truong, A. K. Whittaker, T. P. Davis and K. Peter, *Expert Opin. Drug Delivery*, 2018, **15**(1), 33–45.

62 H. Ye, Z. Shen and Y. Li, *J. Eng. Mech.*, 2019, **145**(4), 04019021.

63 A. Kumar and M. D. Graham, *Soft Matter*, 2012, **8**(41), 10536–10548.

64 B. Czaja, M. Gutierrez, G. Závodszky, D. De Kanter, A. Hoekstra and O. Eniola-Adefeso, *PLoS Comput. Biol.*, 2020, **16**(3), 1–18.

65 M. Cooley, A. Sarode, M. Hoore, D. A. Fedosov, S. Mitragotri and A. Sen Gupta, *Nanoscale*, 2018, **10**(32), 15350–15364.

66 A. J. Thompson, E. M. Mastria and O. Eniola-Adefeso, *Biomaterials*, 2013, **34**(23), 5863–5871.

67 H. Ye, Z. Shen and Y. Li, *Soft Matter*, 2018, **14**(36), 7401–7419.

68 J. K. Tee, M. I. Setyawati, F. Peng, D. T. Leong and H. K. Ho, *Nanotoxicology*, 2019, **13**(5), 682–700.

69 M. I. Setyawati, C. Y. Tay, B. H. Bay and D. T. Leong, *ACS Nano*, 2017, **11**(5), 5020–5030.

70 C. Y. Tay, M. I. Setyawati and D. T. Leong, *ACS Nano*, 2017, **11**(3), 2764–2772.

71 M. I. Setyawati, C. Y. Tay, S. L. Chia, S. L. Goh, W. Fang, M. J. Neo, H. C. Chong, S. M. Tan, S. C. J. Loo, K. W. Ng, J. P. Xie, C. N. Ong, N. S. Tan and D. T. Leong, *Nat. Commun.*, 2013, **4**(1), 1–12.

72 F. Peng, M. I. Setyawati, J. K. Tee, X. Ding, J. Wang, M. E. Nga, H. K. Ho and D. T. Leong, *Nat. Nanotechnol.*, 2019, **14**(3), 279–286.

73 O. Akhavan and E. Ghaderi, *ACS Nano*, 2010, **4**(10), 5731–5736.

74 V. T. H. Pham, V. K. Truong, M. D. J. Quinn, S. M. Notley, Y. Guo, V. A. Baulin, M. Al Kobaisi, R. J. Crawford and E. P. Ivanova, *ACS Nano*, 2015, **9**(8), 8458–8467.

75 Y. Li, H. Yuan, A. Von Dem Bussche, M. Creighton, R. H. Hurt, A. B. Kane and H. Gao, *Proc. Natl. Acad. Sci. U. S. A.*, 2013, **110**(30), 12295–12300.

76 X. Zou, L. Zhang, Z. Wang and Y. Luo, *J. Am. Chem. Soc.*, 2016, **138**(7), 2064–2077.

77 R. Wu, H. Zhang, J. Pan, H. Zhu, Y. Ma, W. Cui, H. A. Santos and G. Pan, *Adv. Mater. Interfaces*, 2016, **3**(18), 1600472.

78 T. Guo, S. Zhuang, H. Qiu, Y. Guo, L. Wang, G. Jin, W. Lin, G. Huang and H. Yang, *Part. Part. Syst. Charact.*, 2020, **37**, 1–6.

79 N. M. Shaalan, T. Yamazaki and T. Kikuta, *Mater. Chem. Phys.*, 2011, **127**, 143–150.

80 S. Mo, Y. Song, M. Lin, J. Wang, Z. Zhang, J. Sun, D. Guo and L. Liu, *J. Colloid Interface Sci.*, 2022, **608**, 2896–2906.

81 C. C. Chang, P. H. Chen, H. L. Chu, T. C. Lee, C. C. Chou, J. I. Chao, C. Y. Su, J. S. Chen, J. S. Tsai, C. M. Tsai and Y. P. Ho, *Appl. Phys. Lett.*, 2008, **93**(3), 033905.

82 J. Fares, M. Y. Fares, H. H. Khachfe, H. A. Salhab and Y. Fares, *Signal Transduction Targeted Ther.*, 2020, **5**, 28.

83 W. Ngwa, O. C. Irabor, J. D. Schoenfeld, J. Hesser, S. Demaria and S. C. Formenti, *Nat. Rev. Cancer*, 2018, **18**, 313–322.

84 I. Morales-Orue, R. Chicas-Sett and P. C. Lara, *Pract. Oncol. Radiother.*, 2019, **24**(1), 86–91.

85 Y. Min, K. C. Roche, S. Tian, M. J. Eblan, K. P. McKinnon, J. M. Caster, S. Chai, L. E. Herring, L. Zhang, T. Zhang, J. M. Desimone, J. E. Tepper, B. G. Vincent, J. S. Serody and A. Z. Wang, *Nat. Nanotechnol.*, 2017, **12**(9), 877–882.

86 Q. Chen, J. Chen, Z. Yang, J. Xu, L. Xu, C. Liang, X. Han and Z. Liu, *Adv. Mater.*, 2019, **31**(10), 1802228.

87 X. Duan, C. Chan and W. Lin, *Angew. Chem., Int. Ed.*, 2019, **58**(3), 670–680.

88 H. Maeda, *J. Controlled Release*, 2012, **164**(2), 138–144.

89 H. Kang, S. Rho, W. R. Stiles, S. Hu, Y. Baek, D. W. Hwang, S. Kashiwagi, M. S. Kim and H. S. Choi, *Adv. Healthcare Mater.*, 2020, **9**, e1901223.

90 E. Blanco, H. Shen and M. Ferrari, *Nat. Biotechnol.*, 2015, **33**, 941–951.

91 L. Zhang, H. Su, H. Wang, Q. Li, X. Li, C. Zhou, J. Xu, Y. Chai, X. Liang, L. Xiong and C. Zhang, *Theranostics*, 2019, **9**(7), 1893.

92 D. Rosenblum, N. Joshi, W. Tao, J. M. Karp and D. Peer, *Nat. Commun.*, 2018, **9**(1), 1410.

93 H. X. Wang, Z. Q. Zuo, J. Z. Du, Y. C. Wang, R. Sun, Z. T. Cao, X. D. Ye, J. L. Wang, K. W. Leong and J. Wang, *Nano Today*, 2016, **11**(2), 133–144.

94 J. A. C. M. Goos, A. Cho, L. M. Carter, T. R. Dilling, M. Davydova, K. Mandleywala, S. Puttick, A. Gupta, W. S. Price, J. F. Quinn, M. R. Whittaker, J. S. Lewis and T. P. Davis, *Theranostics*, 2020, **10**(2), 567.

95 F. Danhier, *J. Control. Release*, 2016, **244**, 108–121.

96 Y. Shi, R. van der Meel, X. Chen and T. Lammers, *Theranostics*, 2020, **10**(17), 7921.

97 H. Cabral, S. Uchida, F. Perche and C. Pichon, *Mol. Pharmaceutics*, 2020, **17**(10), 3654–3684.

98 M. van Dülmen and A. Rentmeister, *Biochemistry*, 2020, **59**(17), 1650–1655.

99 J. Kim, Y. Eygeris, M. Gupta and G. Sahay, *Adv. Drug Delivery Rev.*, 2021, 83–112.

100 Z. Wu and T. Li, *Pharm. Res.*, 2021, **38**(3), 473–478.

101 P. P. G. Guimaraes, R. Zhang, R. Spektor, M. Tan, A. Chung, M. M. Billingsley, R. El-Mayta, R. S. Riley, L. Wang, J. M. Wilson and M. J. Mitchell, *J. Controlled Release*, 2019, **316**, 404–417.

102 R. Verbeke, I. Lentacker, K. Breckpot, J. Janssens, S. van Calenbergh, S. C. de Smedt and H. Dewitte, *ACS Nano*, 2019, **13**(2), 1655–1669.

103 X. Su, J. Fricke, D. G. Kavanagh and D. J. Irvine, *Mol. Pharmaceutics*, 2011, **8**(3), 774–787.

104 Z. Sharifnia, M. Bandehpour, H. Hamishehkar, N. Mosaffa, B. Kazemi and N. Zarghami, *Iran. J. Pharm. Res.*, 2019, **18**(4), 1659–1675.

105 K. Van der Jeught, S. de Koker, L. Bialkowski, C. Heirman, P. Tjok Joe, F. Perche, S. Maenhout, S. Bevers, K. Broos, K. Deswarte, V. Malard, H. Hammad, P. Baril, T. Benvegnu, P. A. Jaffrès, S. A. A. Kooijmans, R. Schiffelers, S. Lienenklaus, P. Midoux, C. Pichon, K. Breckpot and K. Thielemans, *ACS Nano*, 2018, **12**(10), 9815–9829.

106 E. J. Sayour, A. Grippin, G. de Leon, B. Stover, M. Rahman, A. Karachi, B. Wummer, G. Moore, P. Castillo-Caro, K. Fredenburg, M. R. Sarkisian, J. Huang, L. P. Deleyrolle, B. Sahay, S. Carrera-Justiz, H. R. Mendez-Gomez and D. A. Mitchell, *Nano Lett.*, 2018, **18**(10), 6195–6206.

107 Z. Xu, Y. Wang, L. Zhang and L. Huang, *ACS Nano*, 2014, **8**(4), 3636–3645.

108 N. Veiga, M. Goldsmith, Y. Granot, D. Rosenblum, N. Dammes, R. Kedmi, S. Ramishetti and D. Peer, *Nat. Commun.*, 2018, **9**(1), 1–9.

109 A. Padmakumar, N. P. Koyande and A. K. Rengan, *Adv. Ther.*, 2022, 2200042.

110 N. Kong, W. Tao, X. Ling, J. Wang, Y. Xiao, S. Shi, X. Ji, A. Shajii, S. T. Gan, N. Y. Kim, D. G. Duda, T. Xie, O. C. Farokhzad and J. Shi, *Sci. Transl. Med.*, 2019, **11**(523), 1–17.

111 M. A. Islam, J. Rice, E. Reesor, H. Zope, W. Tao, M. Lim, J. Ding, Y. Chen, D. Aduluso, B. R. Zetter, O. C. Farokhzad and J. Shi, *Biomaterials*, 2021, **266**, 120431.

112 T. Yang, C. Li, X. Wang, D. Zhao, M. Zhang, H. Cao, Z. Liang, H. Xiao, X. J. Liang, Y. Weng and Y. Huang, *Bioact. Mater.*, 2020, **5**(4), 1053–1061.

113 M. M. Billingsley, N. Singh, P. Ravikumar, R. Zhang, C. H. June and M. Mitchell, *J. Nano Lett.*, 2020, **20**(3), 1578–1589.

114 L. Miao, L. Li, Y. Huang, D. Delcassian, J. Chahal, J. Han, Y. Shi, K. Sadtler, W. Gao, J. Lin, J. C. Doloff, R. Langer and D. G. Anderson, *Nat. Biotechnol.*, 2019, **37**(10), 1174–1185.

115 X. Zhang, K. Men, Y. Zhang, R. Zhang, L. Yang and X. Duan, *Int. J. Nanomed.*, 2019, **14**, 2733–2751.

116 H. Zhang, X. You, X. Wang, L. Cui, Z. Wang, F. Xu, M. Li, Z. Yang, J. Liu, P. Huang, Y. Kang, J. Wu and X. Xia, *Proc. Natl. Acad. Sci. U. S. A.*, 2021, **118**(6), 1–12.